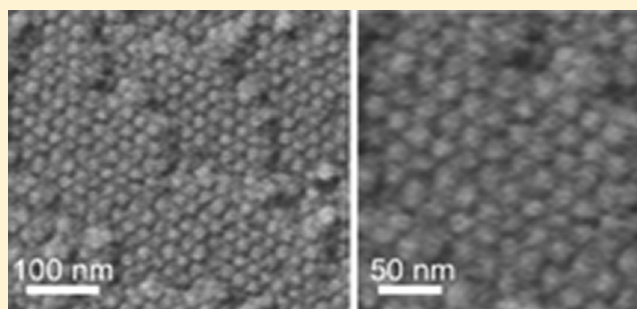


# Nanostructure Formation in the Lecithin/Isooctane/Water System

Naama Koifman, Maya Schnabel-Lubovsky, and Yeshayahu Talmon\*

Department of Chemical Engineering and the Russell Berrie Nanotechnology Institute (RBNI), Technion-Israel Institute of Technology, Haifa 32000, Israel

**ABSTRACT:** We present here for the first time a study of the self-assembled nanostructures in the lecithin/isooctane/water system by direct-imaging techniques, namely, cryogenic transmission electron microscopy (cryo-TEM) and cryogenic scanning electron microscopy (cryo-SEM). Along the dilution line  $[\text{water}]/[\text{lecithin}] = 5$ , we identified a nanostructural development with the increase of lecithin concentration. The system changes from a single reverse micellar phase, through a reverse micellar phase coexisting with a lamellar phase, and finally to a reverse liquid crystalline cubic phase and a lamellar phase. We compared the nanostructures formed when phosphatidylcholine rather than naturally occurring lecithin is used and found that both phase behavior and nanostructure are significantly different. The use of the two complementary cryo-EM techniques proved very efficient in the nanostructural characterization of the system. We also performed small-angle X-ray scattering to confirm our findings. Since the system is very sensitive to changes in composition, the cryo-EM specimens were prepared in a Controlled Environment Vitrification System (CEVS) that has been modified for our specimen preparation needs. We were able to overcome the challenges involved in directly imaging this nonaqueous (oil-rich), concentrated complex liquid systems, thus extending the usefulness of those characterization techniques.



## INTRODUCTION

The complex liquid system of lecithin/isooctane/water shows a large variety of nanostructures, depending on its composition. The oil-rich corner of the system has been extensively investigated due to its unique properties. In that range of compositions, the oil is the continuous medium, inducing the formation of inverted micellar structures, in which the hydrophobic tails of the surfactant point out into the oil and the hydrophilic head-groups point inward into the aqueous environment. Being a double-tailed surfactant, lecithin bears a large hydrophobic portion and therefore tends to form reverse nanostructures when dissolved in organic solvent. This behavior can be predicted by the surfactant parameter,  $N_s = v/la_0$ , where  $v$  is the volume of fully extended hydrophobic tail,  $l$  is the length of the hydrocarbon chains and  $a_0$  is the effective area per headgroup.<sup>1</sup>

The terms “lecithin” and “phosphatidylcholine” (PC) are often used interchangeably. However, naturally occurring lecithin, often extracted from plant seeds, is a complex mixture of phospholipids of various head groups. These phospholipids resemble those comprising cell membranes. Hence, they are biocompatible and have potential applications in drug delivery, cosmetics, and food formulations.<sup>2</sup>

According to several publications,<sup>3–12</sup> a highly viscous, gel-like solution is formed upon the addition of a small amount of water to a mixture of PC and isooctane. The high viscosity was attributed to the formation of reverse threadlike micelles (rTLMs) that entangle, similarly to some polymer molecules in solution. Ternary phase diagrams are normally used to indicate

the regions where such gels exist.<sup>7,13</sup> Shchipunov et al. compared the rheological behavior of the system to that of polymer solutions.<sup>8,14</sup> In both systems, elongated structures form entanglements and a branched network, leading to a dramatic increase in viscosity. Unlike polymer solutions, surfactant threadlike micelles are considered “living polymers”, owing to their reversible nature of self-assembly. The rheological behavior of the system is thus affected, because the system may relax applied shear by breaking and recombination of the TLMs, unlike the behavior of polymeric solutions.<sup>15,16</sup>

Various potential applications of this system have been reported. Peng et al.<sup>11</sup> used lecithin reverse micelles to solubilize proteins in their polar core. They also demonstrated the very strong effect of the phospholipid tail on the solubilization of water in the micelle core. Longer hydrocarbon tails allowed increased solubilization of water. Avramiotis and co-workers used electron paramagnetic resonance (EPR) spectroscopy with membrane-sensitive probes and demonstrated the formation of elongated interfaces by the phosphatidylcholine molecules in hydrocarbon solution upon the addition of minute amounts of water. These elongated interfaces were attributed to the entangled elongated threadlike micelles that make up the gel phase. They solubilized bioactive

Received: June 4, 2013

Revised: July 16, 2013

compounds in the gel, to potentially be used as a transdermal cream.<sup>12</sup>

Mixtures of phospholipids containing a low concentration of phosphatidylcholine do not yield a gel phase.<sup>3</sup> Wolf et al.<sup>17</sup> used a naturally occurring lecithin mixture containing only 25 wt. % phosphatidylcholine and mapped the region where a W/O microemulsion exists, which is approximately at the same composition range indicated by previous work as consisting of reverse threadlike micelles. The microemulsion phase, however, did not exhibit viscoelastic behavior when water was added. In other cases a cosurfactant, such as a short chain alcohol was added to form a microemulsion that solubilized proteins in its polar core.<sup>18</sup> A change in viscosity was observed only upon a significant increase in lecithin concentration, when the solution turned into a thick gel.

The reported studies of lecithin/oil/water systems were performed using a variety of techniques, including light scattering,<sup>4</sup> small-angle X-ray scattering (SAXS),<sup>13</sup> small-angle neutron scattering (SANS),<sup>7</sup> self-diffusion NMR,<sup>17</sup> electron paramagnetic resonance,<sup>12</sup> cross-polarized microscopy,<sup>7,13</sup> and rheology measurements.<sup>6–8,13,14,19</sup> The oils in the systems were mainly *n*-decane,<sup>14,19</sup> cyclohexane,<sup>9</sup> and isooctane.<sup>3,7,13</sup> Except for one documented case of room temperature TEM for the lecithin/benzene/water system,<sup>20</sup> no electron microscopy was carried out on those systems.

Since this is a complex liquid system sensitive to changes in composition and temperature, room-temperature TEM is an ill-suited characterization technique.<sup>21</sup> Electron microscope specimen preparation under controlled conditions by thermal fixation is effective for the preservation of structures in solution, and for imaging under cryogenic conditions in a TEM<sup>22</sup> or an SEM.<sup>23</sup> Most cryo-EM studies were performed on water-continuous systems due to their abundance in nature. Some nonaqueous liquid systems were imaged by cryo-TEM,<sup>24–27</sup> but each system required fine-tuning of specimen preparation and imaging.

In this work we set out to characterize some of the regions of the lecithin/isooctane/water phase diagram by means of cryogenic transmission electron microscopy (cryo-TEM), cryogenic high-resolution scanning electron microscopy (cryo-HR-SEM), and small-angle X-ray scattering (SAXS). Our study is yet another example of the usefulness of cryo-EM in characterization of complex liquid systems, even oil-continuous ones.

## ■ EXPERIMENTAL SECTION

**Materials.** Soybean lecithin in a granular form was purchased from Acros Organics, USA, with a purity of 97%, and an average molecular weight of 750 g/mol. It was used without further purification. This lecithin is a mixture of phospholipids of the roughly following composition: 25% phosphatidylcholine (PC), 20% phosphatidylethanolamine (PE), 15% phosphatidylinositol (PI), 9% phosphatidic acid, 8% other phospholipids, 8% sugars, 15% glycolipids, 3% triglycerides, and 1% moisture. The fatty acids chains in the phospholipids are made of about 20% saturated, 17% monounsaturated, and 62% polyunsaturated fatty acids, and 1% other fatty acids. Purified phosphatidylcholine (Emulmetik 390) was a generous gift from Lucas Meyer. It contains approximately 95% pure phosphatidylcholine and has a molecular weight of about 800 g/mol. It, too, was used as received without further purification. The fatty acids comprising its tails were made of about 20% saturated, 10% monounsa-

turated and approximately 70% polyunsaturated fatty acids. Chain length of the tails in both lecithin types was between 16 and 18 carbons. Isooctane (2,2,4-trimethylpentane) was purchased from Sigma, USA, with a purity of 99% and density of 0.692 g/mL at 25 °C. The water used was purified by a Millipore, Milli-Q Plus purification system to a resistivity of 18.2 MΩcm.

**Methods.** Solutions were prepared by mixing the lecithin in the appropriate amount of isooctane for approximately 2–3 h, until the lecithin was fully dissolved. Then water was added and the solution was shaken or stirred overnight. To allow for complete dispersion of the water in the solution, the mixture was vortexed after the addition of the water. Time zero ( $t = 0$ ) was set after overnight stirring of the sample. The sample was then stored in a water bath at  $25 \pm 0.5$  °C and kept in the dark to minimize lecithin photo-oxidation.

Cryogenic transmission electron microscopy (cryo-TEM) imaging was performed either by a Phillips CM120 or an FEI Tecnai T12 G<sup>2</sup> electron microscopes, operated at an accelerating voltage of 120 kV. Specimens were transferred into an Oxford CT-3500 cryo-holder (Philips) or a Gatan 626DH (FEI) cryo-holders, and equilibrated below  $-178$  °C. Specimens were examined using a low-dose imaging procedure to minimize electron-beam radiation damage. Images were recorded digitally by a Gatan Multiscan 791 cooled CCD camera (Philips CM 120), or a Gatan US 1000 high-resolution CCD camera (Tecnai T12 G<sup>2</sup>), using the DigitalMicrograph software.

Cryo-TEM specimens were prepared in a controlled environment vitrification system (CEVS).<sup>28</sup> Aqueous system specimens are usually prepared in this temperature-controlled chamber with humidity at saturation to prevent evaporation from the specimens. In our case, most of the samples contained mostly isooctane, and therefore isooctane was used to saturate the air inside the CEVS chamber. A drop of the solution was placed on a carbon-coated perforated polymer film, supported on a 200 mesh TEM grid, mounted on a tweezers. The drop was turned into a thin film (preferably less than 300 nm) by blotting away excess solution with a metal strip covered with a filter paper. The grid was then plunged quickly into liquid nitrogen at its boiling point ( $-196$  °C). Although liquid nitrogen is a poor cryogen (compared to liquid ethane at its freezing point), it can still vitrify branched hydrocarbons such as isooctane, which is used in this case.<sup>25</sup> Liquid ethane is not used here because it dissolves the organic solvent. All the isooctane-rich specimens were quenched from 25 °C and a saturated environment of isooctane.<sup>22,29</sup>

Cryogenic scanning electron microscopy (cryo-SEM) imaging was performed with a Zeiss Ultra Plus high-resolution SEM, equipped with a Schottky field-emission electron gun and with a BalTec VCT100 cold-stage maintained below  $-145$  °C. Specimens were examined at very low acceleration voltage from 1 to 3 kV, and short working distances of 2.5–5 mm. Working conditions were adjusted according to the type of sample and preparation conditions, to optimize high resolution imaging. We used both the in-the-column (“InLens”) and the Everhart Thornley (“SE2”) secondary electron imaging detectors.

Specimens were prepared in the CEVS from a temperature of 25 °C and saturation of isooctane (for the oil-rich samples). A drop of the solution was “sandwiched” between two gold planchettes and fixed inside a specialized set of tweezers. The tweezers were then rapidly plunged into liquid nitrogen at its boiling point ( $-196$  °C), and the sandwich was inserted into a

“sample-table” which was also cooled in liquid nitrogen. The sample table was then transferred into a BAF060 freeze-fracture system (BalTec AG, Liechtenstein), a high vacuum system, where it was set on a cooled stage at a temperature of  $-170$  to  $-180$  °C. In the BAF060 chamber, the sandwiches were split open to fracture the frozen specimen. The fractured surfaces were then coated with a 4 nm layer of platinum–carbon (Pt–C) at a  $90^\circ$  angle, to increase the electric conductivity of the specimen, and decrease charging effects by the electron beam. The coated specimens were then transferred under vacuum and cryogenic temperature by a BalTec VCT100 shuttle, precooled with liquid nitrogen, to the precooled stage of the HR-SEM for imaging. This methodology is described in detail by Issman and Talmon.<sup>23</sup>

Small-angle X-ray scattering (SAXS) was performed using a small-angle diffractometer (Molecular Metrology SAXS system) with Cu  $K\alpha$  radiation from a sealed microfocus tube (MicroMax-002+S), two Göbel mirrors, and three-pinhole slits. The generator was powered at 45 kV and 0.9 mA. The scattering patterns were recorded by a  $20 \times 20$  cm two-dimensional position sensitive wire detector (gas filled proportional type of Gabriel design with  $200 \mu\text{m}$  resolution), positioned 150 cm behind the sample. The resolution of the SAXS system is about  $3 \times 10^{-2} \text{ nm}^{-1}$ . The scattered intensity  $I(q)$  was recorded at  $0.07 < q < 2.7 \text{ nm}^{-1}$ , where  $q$  is the scattering vector defined as:

$$q = (4\pi/\lambda) \times \sin(\theta)$$

where  $2\theta$  is the scattering angle and  $\lambda$  is the radiation wavelength ( $\lambda = 0.1542 \text{ nm}$ ).

The scattering intensity,  $I(q)$ , was normalized to the following parameters: time, solid-angle, primary beam intensity and capillary diameter. Scattering of the solvent (isooctane), empty capillary and electronic noise were subtracted.

## RESULTS

Using direct imaging techniques, namely, cryo-TEM and cryo-SEM, we were able to show the structural nature, on the nanoscale, as a function of concentration and type of lecithin. The investigation focused mainly on the oil-rich side of the phase diagram of the ternary system lecithin/isooctane/water. On the basis of previous reports,<sup>9,13,17</sup> we expected a transition in nanostructure with the change in composition. We were also able to visualize, for the very first time, the striking difference in nanostructure between a system containing a mixture of phospholipids and a system that contains pure phosphatidylcholine. Although both types are often referred to as simply “lecithin”, the differences in nanostructural behavior, contradict this notion. In both cases, reverse structures formed due to the excess of isooctane, which formed the continuous phase, but the nature of these nanostructures is different, which was also evident in the nature of the solution on the macro scale.

All samples were homogeneous over the time of the study, on the micrometric level. In some cases small amounts of precipitate, probably a result of lecithin impurities, were formed. Our sampling avoided the precipitate.

**Naturally-Occurring Lecithin/Isooctane/Water System.** Initially we looked at the naturally occurring lecithin system, along a “dilution line” of constant water to lecithin molar ratio ( $W_0$ ).<sup>30,31</sup> Along the dilution line of  $W_0 = 5$  we examined 4 samples whose concentrations are shown in Figure 1. We also present here one sample that is water-rich, as it, too, corresponds to a liquid crystalline phase. Most solutions were

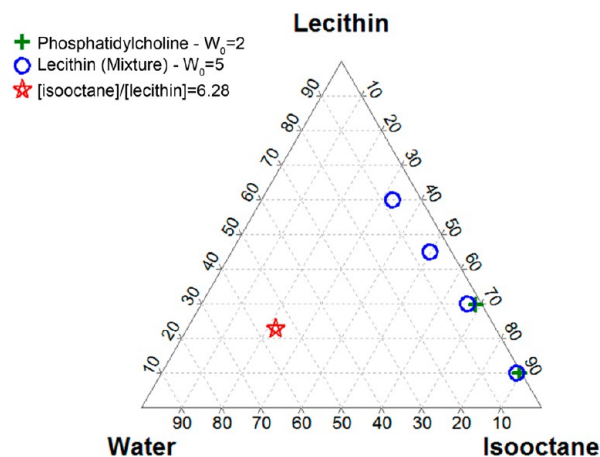


**Figure 1.** Ternary diagram of the system soybean lecithin/isooctane/water. Concentrations are given in weight percent. Different symbols indicate different dilution lines; the crosses belong to solutions containing PC.

examined at  $t = 0$ , that is, the next day after preparation. Then they were examined again after a few months, and several were examined again more than a year later.

The main structures we observed in the oil-rich corner samples were spheroidal reverse micelles. No major change in nanostructure was observed upon the increase in lecithin concentration, until reaching concentrations as high as 45% and 60% wt. lecithin. At those concentrations we detected a lamellar phase by cryo-SEM.

The sample with the lowest content of lecithin and water is sample No. 1, with 10/88.8/1.2 wt.% lecithin, isooctane and water, respectively. In Figure 2 we present the nanostructures we observed in this solution at different times from preparation. At  $t = 0$  (Figure 2A, B), we identified reverse spheroidal

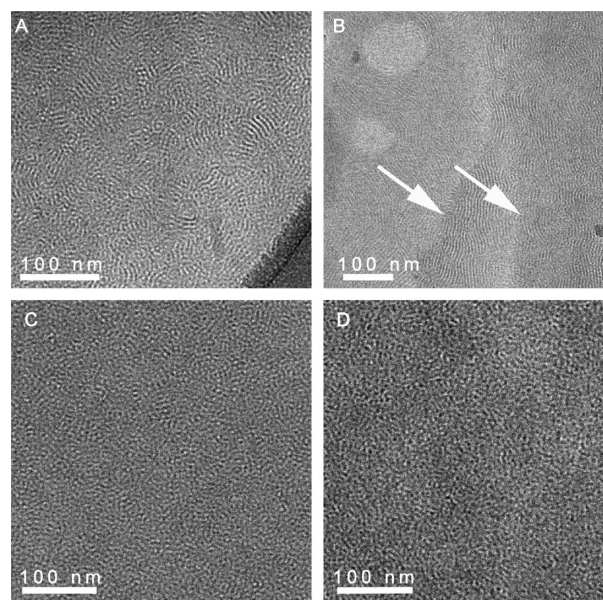


**Figure 2.** Cryo-TEM micrographs of sample No. 1. (A, B) At  $t = 0$ ; spheroidal and elongated reverse micelles are visible. Arrows in B indicate differences in optical density corresponding to superposed layers in the specimen. (C) At 1 month, shorter structures and a lower degree of order are evident. (D) At 9 months, only spheroidal micelles are observed; there seems to be no interaction or order of the micelles.



micelles and elongated structures, which we first suspected were reverse threadlike micelles (rTLMs). However, we ruled out the existence of superimposed rTLMs by the SAXS results (see below). The different optical densities areas observed in Figure 2B (white arrows) correspond to superposed layers. After one month we saw mostly shorter aggregates, such as reverse spheroidal micelles (Figure 2C). Similar structures were observed after 9 months (Figure 2D).

Sample No. 2, somewhat more concentrated in lecithin, contained 30/66.4/3.6 wt. % of lecithin, isooctane and water. In this solution, we identified behavior similar to that of sample No. 1. At  $t = 0$ , there was a mixture of short reverse structures and more elongated ones. The degree of order here seems higher (Figure 3A). After three months, there was a lower

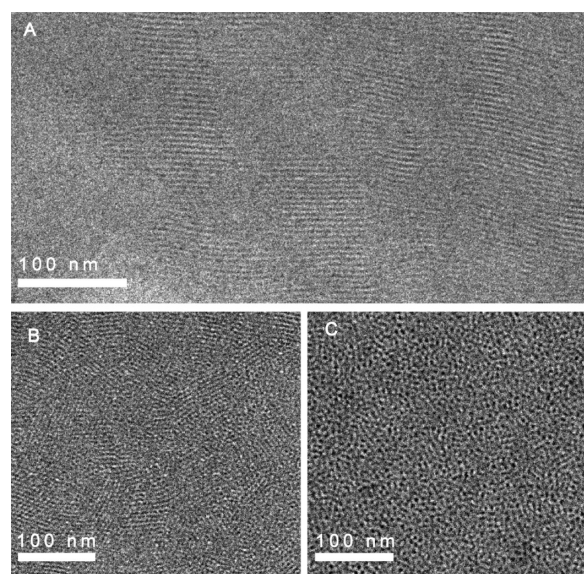


**Figure 3.** Cryo-TEM micrographs of sample No. 2. (A) At  $t = 0$ ; an organized elongated structure, possibly rTLMs. (B) At 3 months; a lower degree of order of spheroidal reverse micelles. (C) After 1 year; only spheroidal reverse micelles are observed with no significant degree of intermicellar order.

degree of order, and we observed mostly reverse spheroidal micelles (Figure 3B). After one year, we found no evidence for any order of the spheroidal reverse micelles, containing water in their core.

To complete the characterization of the nanostructure and to rule out artifacts, we also used small-angle X-ray scattering. SAXS was performed on sample No. 1 and No. 2 at  $t = 0$  (Figure 4). The spectra of sample No.1, the most diluted sample examined at  $W_0 = 5$ , showed a peak around  $q = 1.45 \text{ nm}^{-1}$ , and very minor peak of structure factor, at small angles, at  $q = 0.42 \text{ nm}^{-1}$ . The peak at larger angles is related to the form factor, and was fit to a model of spheroidal micelles (Figure 4A). We found an excellent fit between the model and the experimental results. The minor peak at the low angles is attributed to a minor structure factor and indicates a small degree of intermicellar interaction at that concentration. Comparing these results to the cryo-TEM micrographs of Figure 2, we conclude that the solution contains reverse spheroidal micelles, and that the elongated structures could have resulted from specimen preparation (see Discussion).

Solution No. 2, showed two distinct peaks, at  $q = 0.67 \text{ nm}^{-1}$  and  $q = 1.44 \text{ nm}^{-1}$ . The position of the second peak is almost

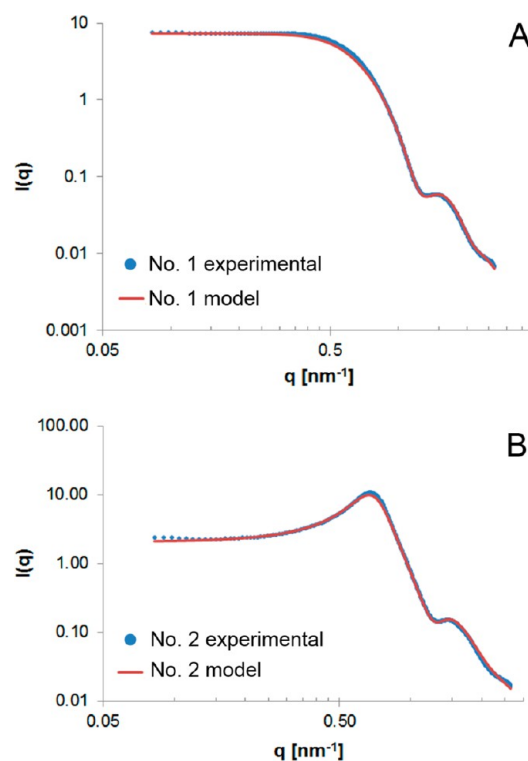


**Figure 4.** SAXS spectra of solution No. 1 (A) and No. 2 (B); experimental results (blue ●) and the model fit (red —).

the same as in solution No.1, and similarly it fit very well the sphere model. The structure factor peak, however, was strong and distinct (Figure 4B). This may be attributed to the increased concentration of lecithin, which leads to a higher concentration of densely packed micelles, leading to more pronounced interaction. The structure factor was fit to the “hard-sphere” model, in which the micelles are modeled as hard, perfectly elastic balls.<sup>32,33</sup> That means the micelles remain spheroidal as the concentration is increased, and pack closer together, as seen in Figure 3B. These results agree with our observations of mostly spheroidal reverse micelles in the above solutions. The mean size of the micelles extracted from the SAXS measurements is 3.79 nm for sample No. 1, and 3.77 nm for sample No. 2. The similar micelle size is logical, since the samples are on the same dilution line, on which the water to lecithin ratio remains constant, thus not affecting the size of the micelles.

Sample No. 3 is more concentrated with lecithin and water, and yet it is still liquid, and a dramatic increase in viscosity is not observed upon addition of water. However, since it is more concentrated and somewhat more viscous, it is also a good candidate for cryo-SEM imaging. The results shown in Figure 5 exhibit complementarity of cryo-SEM and cryo-TEM data. Cryo-TEM allows imaging of nanometric structures, while specimen preparation often excludes larger structures that may not fit in the thin specimen, only tens to a few hundreds nanometers thick. In cryo-SEM, specimen thickness can reach several millimeters; relatively large structures are therefore not excluded. In cryo-TEM we obtain a two-dimensional projection image of the three-dimensional specimen. Therefore, we cannot extract any topographical information from TEM micrographs. Topographical information is easily obtained in the SEM, as can be seen in Figure 5B and C. Because in the SEM the picture is formed by the Everhart Thornley detector by secondary and

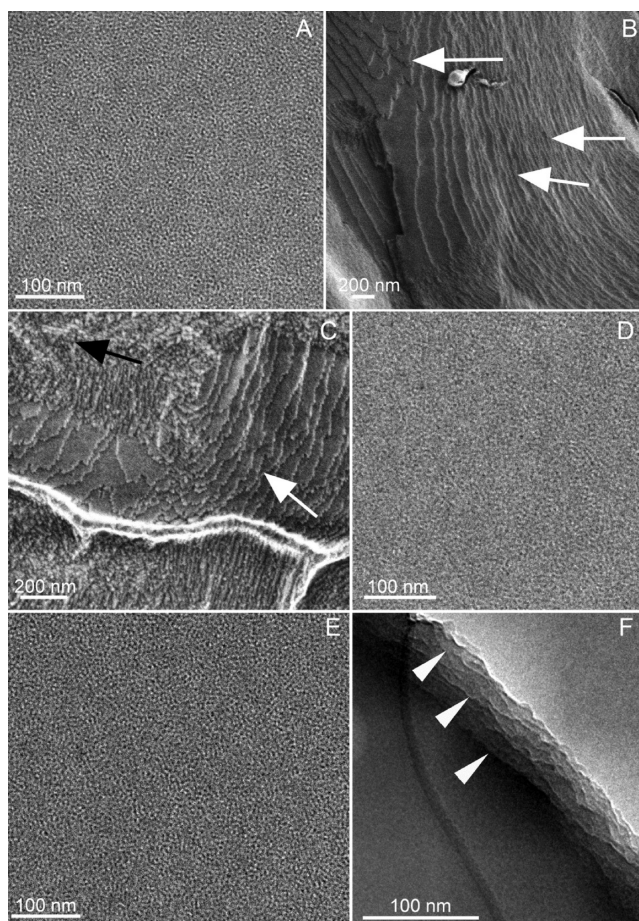


**Figure 5.** Sample No. 3: (A) cryo-TEM at  $t = 0$ ; spheroidal reverse micelles; (B, C) cryo-SEM at 1 month; a mixture of lamellar phase (white arrows) and short reverse micelles (black arrow); (D) cryo-TEM at 6 months; spheroidal reversed micelles; (E, F) cryo-TEM at 16 months; a mixture of reverse micellar phase (E) and lamellar phase (arrowheads pointing to layer edge; F).

backscattered electrons, we obtain detailed information of surface topography.

We imaged the solution at  $t = 0$ ,  $t = 1$  month,  $t = 6$  months and  $t = 16$  months, and identified in the micrographs some regions that are arranged in a lamellar phase, and some other regions of reverse spheroidal micelles. The development with time is shown in cryo-TEM and cryo-SEM micrographs (Figure 5). At  $t = 0$  (Figure 5A) we see spheroidal micelles similar to the ones observed in the more diluted samples of the same  $W_0$ . After one month a well-defined lamellar phase is seen: In Figure 5B and 5C one notices the step-like structure of bilayers. Notice also the different orientations of the lamellae indicated by the white arrows. In the top-left corner of Figure 5C the lamellar phase changes into a different phase, most probably a reverse micellar structure, as the one seen in the cryo-TEM micrographs. At 6 months and after 1 year and 4 months (Figure 5D–F) we observed the same structures. However, at the edges of the film of the cryo-TEM specimen, we noticed a layered structure (arrowheads), which indicates the presence of both phases in solution.

Cryo-TEM was very effective to image dilute solutions of higher concentration of isooctane and lower concentrations of lecithin. However, when the concentration of structures is high, it is difficult to identify the real structures in solution, without

the help of another imaging technique, electron tomography or an indirect method. In addition, at an elevated concentration of lecithin, there is a sharp increase in solution viscosity, and a very viscous, transparent gel is formed, as we observed in sample No. 4. Such a gel cannot be made into a thin film of about  $\sim 100$ – $300$  nm and therefore cannot be imaged by cryo-TEM. The use of cryo-SEM in this case is very useful.

Sample No. 4 on dilution line  $W_0 = 5$  contains 60/32.8/7.2 wt.% of lecithin, isooctane and water. The solution is highly viscous, transparent gel. The dense lamellar structure is evident throughout it (Figure 6A and B). However, SAXS experiments

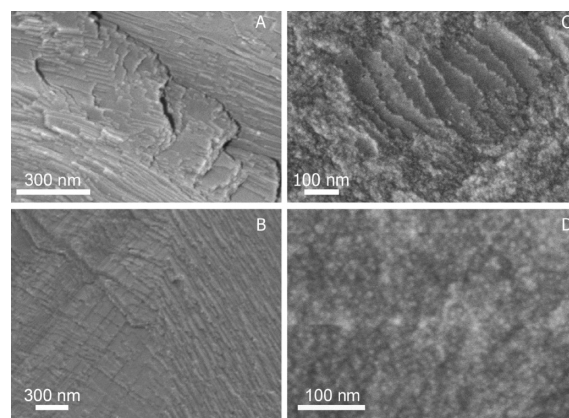


**Figure 6.** Sample No. 4 at  $t = 0$ , imaged by cryo-SEM: (A) the bilayers are shown very clearly; (B) the lamellae are oriented in different directions; (C) a micellar and a lamellar phase coexist; (D) a high magnification image of the densely packed micellar phase.

indicated the existence of another liquid crystalline phase, possibly a cubic one (Figure 7). The first six observed Bragg peaks, except for the second peak at  $q = 0.104 \text{ \AA}^{-1}$ , are permitted reflections of the face-centered cubic  $Fd\bar{3}m$  space group ( $Q^{227}$ ). The relevant Miller indices are therefore  $hkl = 111, 220, 311, 222, 400, 331$ . We obtained the lattice parameter  $a = 12.3$  nm from plotting the reciprocal  $d$  spacings of the observed reflections versus  $(h^2 + k^2 + l^2)^{1/2}$  (Figure 7B). The linearity of the plotted trend-line, as well as its intersection at the axes origin, indicate the validity of the space-group assignment. The remaining peak at  $q = 0.104 \text{ \AA}^{-1}$  is assigned to the lamellar phase, which is observed clearly by cryo-SEM. Figure 6C and D shows a micellar structure that is evident throughout the sample, coexisting with the lamellar phase. The combination of techniques allowed the characterization of this mixture of phases. The reverse micellar cubic phase of space group  $Fd\bar{3}m$  has been reported before in other systems, including block copolymer systems and phospholipid systems.<sup>34–38</sup>

The results along dilution line  $W_0 = 5$  show interesting development, with the increase of lecithin concentration. The change is evident both in nanostructure and macroscopic phase behavior.

**Threadlike Micelles of Phosphatidylcholine.** Because the lecithin used in most of this study was a mixture of phospholipids we wanted to image the nanostructures in a pure phosphatidylcholine system. The differences in viscoelasticity, and phase behavior were drastic, as previously reported by Scartazzini and Luisi.<sup>3</sup> We examined the system PC/isooctane/water in two compositions, 10/89.55/0.45 wt. % (A) and 30/68.5/1.5 wt. % (B), both are approximately on dilution line  $W_0$



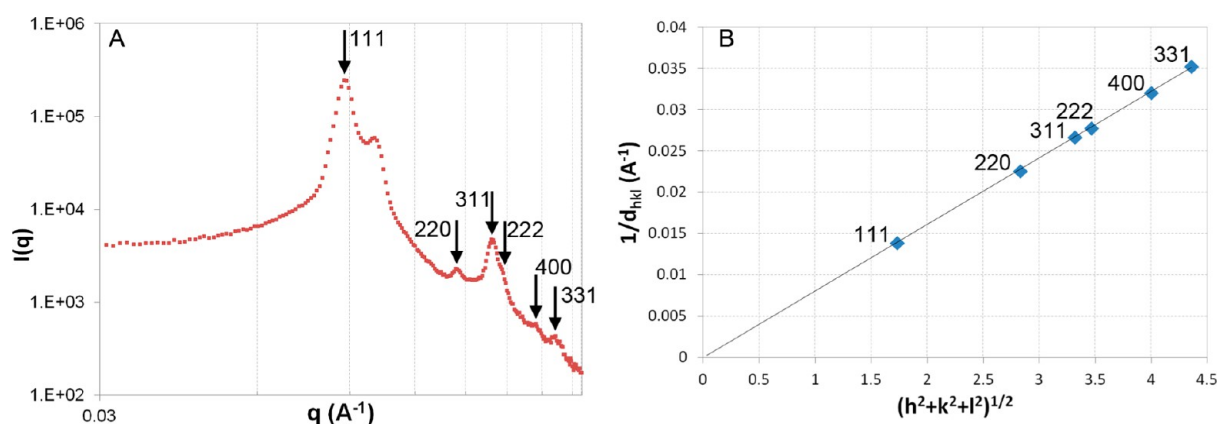


**Figure 7.** (A) SAXS pattern obtained from gel phase of 60/32.8/7.2 wt % lecithin, isoctane and water at 25 °C. The arrows mark the positions of the observed reflections that match the reflections of the  $Fd\bar{3}m$  space-group, suggesting the existence of a reverse micellar cubic phase. The remaining peak (at  $q = 0.104\text{\AA}^{-1}$ , no arrow) is attributed to a lamellar phase coexisting with the cubic phase in the gel. (B) Plot of the reciprocal  $d$ -spacings of the reflections marked in (A). The graph is linear and intercepts (0,0), thus validating the space-group assignment.

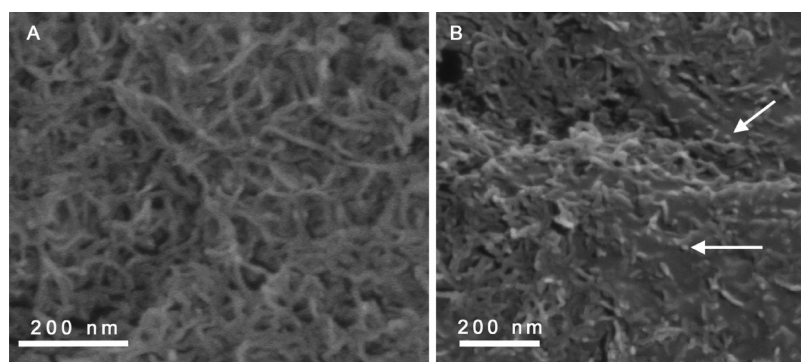


**Figure 8.** Entangled network of rTLMs in sample A imaged by cryo-SEM. (A) High contrast image due to the sublimation of isoctane; (B) rTLMs are embedded in the continuous isoctane. The bright end-caps are discernible (white arrows).

$= 2$ . We chose these compositions since they were found in the single phase region. Upon the addition of water, the solution of lower PC concentration turned highly viscous and transparent, while the second solution of higher PC concentration formed a viscous, highly elastic, transparent gel. We imaged both samples by cryo-SEM and noticed nanostructures that fit perfectly with the macroscopic behavior of the samples.

The first most striking feature that can be seen in sample A (Figure 8) are long highly entangled rTLMs. The entanglements are clearly visible due to the sublimation of isoctane inside the microscope during imaging at a temperature of  $-145\text{ }^{\circ}\text{C}$ , as previously reported by Ben-Barak and Talmon.<sup>39</sup> The cores of the micelles are hydrated with water, which, once frozen, has a very low vapor pressure at cryogenic temperatures (see discussion), and stabilizes the nanostructures during imaging. In Figure 8B, we show an area where isoctane has not fully sublimated and the embedded rTLMs are showing, as their end-caps appear brighter due to higher efficiency of secondary electrons production at edges in SEM imaging. This confirms that these are indeed rTLMs and not drying artifacts as one may suspect.

In sample B, which is more concentrated with PC, the rTLMs do not seem longer but rather more densely packed than the rTLMs of sample A (Figure 9A). This fits our expectations, since the samples fall approximately on the same dilution line, in which the ratio of water to lecithin is constant, thus, fixing the rTLM length.<sup>8,14</sup> In addition, in several regions of the specimen the micelles appear oriented to one direction,

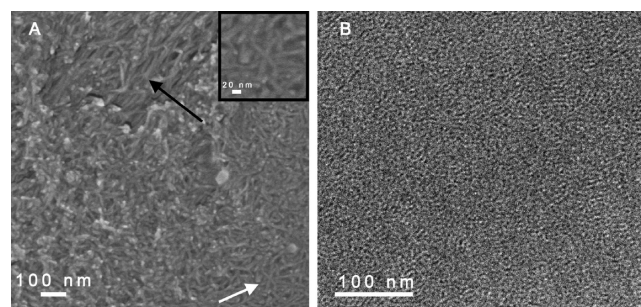


**Figure 9.** (A) Cryo-SEM image of sample B (30/68.5/1.5 wt. % PC/isoctane/water) showing packed rTLMs. Black arrow points to oriented region. White arrow points to an entangled region of several micelles (enlarged view in inset). (B) Cryo-TEM image of sample B (30/68.5/1.5 wt. %) composed of naturally occurring lecithin. Short reverse micelles are evident throughout the image.

which may be a result of shear applied on the sample during specimen preparation.

We compared the systems containing PC and naturally occurring lecithin, containing only 25 wt. % of PC. A sample of the same composition as sample B, containing naturally occurring lecithin, did not exhibit any viscosity change upon water addition, and consequently formed only spheroidal reverse micelles (Figure 9B). The solution was imaged by cryo-TEM only, due to its low viscosity and size of the micelles, which is more compatible for TEM rather than SEM imaging.

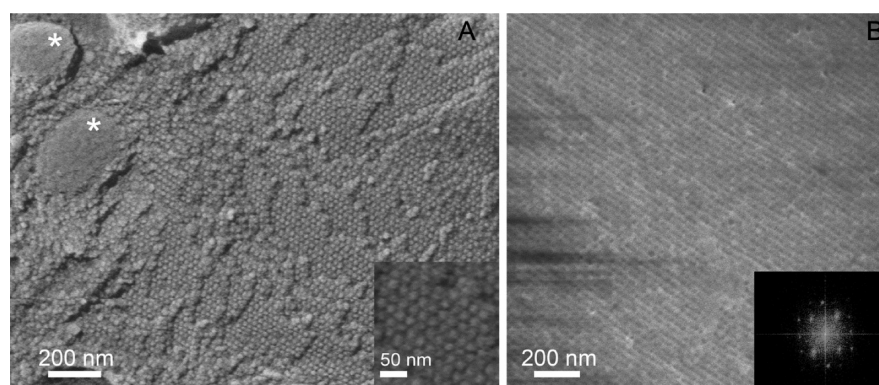


**Figure 10.** Sample No. 5. (A) Cryo-SEM image of a cubic arrangement of micelles in the sample (inset), large vesicles are present on the top left corner of the image (asterisks). (B) Cryo-SEM image of a cubic pattern of cavities that contained micelles plucked out by the fracture; an FFT pattern of it (inset).

**Micellar Cubic Phase at the Water-Rich Corner.** At the water-rich side we investigated the solutions in a region that had been reported to contain hexagonal, lamellar and cubic structures. In the work of Angelico et al.,<sup>13</sup> who used purified phosphatidylcholine, the cubic phase could not be identified clearly, due to the ambiguity of the SAXS measurements. We show here for the first time the formation of a cubic phase of the composition 22/23/55 wt. % of naturally occurring lecithin, isooctane and water, respectively (Sample No. 5). It is worth noting that the lecithin used here is of different composition than the one used by Angelico et al.<sup>13</sup>

All imaging was done by cryo-SEM, because the sample was too viscous for cryo-TEM specimen preparation. Figure 10 shows a cubic arrangement of micelles. Those are most probably swollen micelles with hydrophobic cores, filled with isooctane in a water-continuous matrix. We identified another phase that coexists with the cubic phase in this composition. That phase consists of large vesicles, which are known to form by lecithin in water. The solution is a whitish paste, which indeed suggests that it contains objects larger than micelles. Figure 10A shows a close-packed arrangement of micelles that was fractured in an angle that reveals the packing in a three-dimensional layer-by-layer manner. In this image the micelles remained intact in their position, while the solvent around them, presumably water, had been slightly sublimed and exposed them. In Figure 10B, we show a case where a “negative” image of the ordered micelles has formed. Instead of swollen micelles, we see the arranged pattern as holes. This could have formed in two possible ways. Either, the micelles were removed by the fracture, leaving only craters behind, or the isooctane in the micelles cores sublimed while being imaged in the microscope. The inset in Figure 10B shows a Fast Fourier Transform (FFT) pattern of the image, emphasizing the high symmetry in the sample.

## DISCUSSION

Several articles reported that upon the addition of as little as two water molecules to each lecithin molecule, in the binary solution of lecithin and isooctane, a major viscosity increase takes place by the formation of an organogel.<sup>3,7,10,12,13</sup> This increase in viscosity was attributed to the formation of long threadlike micelles, and their entanglement at higher concentration of water.<sup>8</sup> We did not observe such a change in viscosity in the naturally occurring lecithin based system. We did not image entangled networks throughout the concen-

tration range we investigated. These results are consistent with the investigation by Wolf et al., who also used a naturally occurring lecithin, composed of a mixture of phospholipids.<sup>17</sup> Since the lecithin contains 25% of PC, 20% of PE, 15% of PI, and minor amounts of other phospholipids, the packing parameters are bound to be different from the ones expected in pure PC. Ethanolamine resembles the chemical structure of choline, except that the terminal amine group carries three hydrogen atoms, not three methyl groups as in choline. Inositol is a 6-fold alcohol of cyclohexane of a neutral charge. PI is therefore an anionic amphiphile that can readily interact electrostatically with other molecules. These differences in chemical composition strongly affect the packing parameters of the different phospholipids at the interfacial layer. Both PI and PE head-groups readily form hydrogen bonds. In terms of surface area of head-groups the order is  $PI > PC > PE$ , which means that the molecular shapes are different for each of the phospholipids. PI has a truncated cone shape, PC a cylindrical shape, and PE a reversed cone shape, where the hydrophobic region is significantly larger than the hydrophilic region. This combination of packing properties is less likely to result in the formation of elongated structures such as rTLMs. Instead, short, spheroidal structures are formed.

The formation of multiple phases is possible, as evident throughout the study. Using a mixture of phospholipids increases the complexity of the system and its number of degrees of freedom. Of course, the cheaper, naturally occurring mixture, is readily available, and does not require any further treatment to form the structures presented here. The use of a mixture proves useful in some applications, such as in dermal drug delivery, where the addition of PE significantly improves skin permeation of the drug.<sup>40</sup> In a different study, crude soybean lecithin was superior to pure PC in the formation of microemulsions serving as nanoreactors for the formation of BaSO<sub>4</sub> nanoparticles.<sup>41</sup>

To examine the changes in viscosity upon the addition of water to the binary solution of lecithin and isooctane we measured the relative viscosity of the different solutions using an Ubbelohde viscometer. The experimental details are described elsewhere.<sup>31</sup> We examined 5 solutions of increasing  $W_0$  and measured the flow time through the viscometer. The changes in flow time with the increase of  $W_0$  were negligible, which agrees with our visual observations that no significant changes in viscosity occur upon water addition. The viscosity of the system did eventually increase with the significant increase

of lecithin concentration, forming a thick transparent gel. A thick, viscous, milky system was also evident in the water-rich region, as described above.

An entangled network of rTLMs was, however, clearly visible in the system containing only PC (Figures 8 and 9), which also exhibited the expected viscoelasticity with the addition of water. This emphasizes the major differences between the two systems, both macroscopically and nanoscopically. We examined this system at only two concentrations on the same dilution line. The increase in lecithin concentration has an effect on the entanglements concentration rather than on the structural features of the rTLMs. This is observed both in the cryo-SEM images and in the viscosity of the solutions, which increases with the increase in PC concentration. According to previous publications, the dilution line we studied ( $W_0 = 2$ ) was in the linear growth zone, where the rTLMs are entangled but not yet branched.<sup>6–8,14</sup> However, based on the current results, we cannot yet determine unambiguously whether the micelles are branched or just entangled.

Although isooctane vitrifies well in liquid nitrogen, we should be cautious with the use of isooctane in cryogenic temperatures and high vacuum, the conditions during cryo-TEM and cryo-SEM imaging. In a calculation we performed, using the Antoine's equation, an extrapolation of the vapor pressure of isooctane to cryogenic temperatures showed that its vapor pressure at  $-150\text{ }^\circ\text{C}$  is  $5.6 \times 10^{-11}$  mbar, 7 orders of magnitude higher than that of water at the same temperature,  $9.4 \times 10^{-18}$  mbar. This means that the rate of sublimation at the high vacuum of the microscope and at a temperature as low as  $-150\text{ }^\circ\text{C}$  is significant, and therefore imaging should be done rapidly to capture the nanostructures, before they change due to freeze-drying effects. Sublimation can be advantageous at times: as the continuous phase of isooctane sublimates, it enhances the contrast of the sample, as it exposes the nanostructures in the oil, as seen in Figures 5 and 6.<sup>39</sup>

The use of direct-imaging techniques for this oil-rich lecithin-based system allowed us to witness for the first time the complex phase behavior and its direct relation to the nanostructures formed. The elongated structures observed in the system (Figure 2B and Figure 3A) were probably shear-induced structures formed during cryo-TEM specimen preparation.<sup>42</sup> Cryo-SEM specimen preparation should be done carefully, avoiding drying artifacts. Therefore, the preparation chamber was saturated with isooctane, preventing the evaporation of sample. The combination of cryo-EM methodologies confirmed the findings, and provided additional information about the phases and their nanostructure. In some cases we observed coexisting phases, emphasizing the inhomogeneity at the nanoscale. Although the system appeared isotropic at certain compositions, an investigation by direct-imaging proved otherwise.

At the oil-rich corner the system was comprised of reverse spheroidal micelles, and thus exhibited a Newtonian phase behavior, as its viscosity remained relatively low even at lecithin concentrations as high as 45% wt. No consistent pattern of evolution with time was evident in any of the investigated solutions. Angelico et al.<sup>13</sup> previously suggested that the time for reaching equilibrium in the system of PC/isooctane/water is longer than one year.

## CONCLUSIONS

We reported here direct-imaging of reverse micelles in a nonaqueous solvent. The methodology we developed overcame

many of the challenges encountered in this unique complex liquid system. Unlike many indirect characterization methods, cryo-EM is not a model-dependent technique, producing images that reflect directly the system structure, and therefore it is the method of choice in our study.

We suggest a development of nanostructure along dilution line  $W_0 = 5$ . At low concentration, naturally occurring lecithin self-assembles into short reverse micelles, presumably spheroidal, that grant the solution Newtonian behavior. These nanometric structures were observed mostly by cryo-TEM because of its high resolution and good contrast. As the concentration of lecithin is increased, so does the intermicellar interaction, as evident by SAXS, and the coexistence with a lamellar phase is shown. At high lecithin concentration (60 wt. %), the micellar phase forms a reverse micellar discontinuous-cubic phase, which coexists with a lamellar phase. This was clearly visible by cryo-SEM, while SAXS provided quantitative information. On the water-rich side, we observed a discontinuous micellar cubic phase, of spheroidal micelles, which emphasizes the diversity of structures that are highly composition dependent.

Finally, the use of PC-based system exhibited a viscoelastic phase behavior and the existence of entangled rTLMs. Many studies used this type of solutions, but this is the first time such an entangled network is directly imaged. This comparison was vital to our study, to confirm that indeed there is a major impact to the composition of the lecithin used. It is important to emphasize that the name "lecithin" should be used with care, since it does not always stand for the same substance and composition.

This work underlines the complementarity of cryo-SEM and cryo-TEM. The combination with indirect methods is necessary for full characterization of complex liquid systems. Our direct observations of these unique nanostructures lead to a more thorough understanding of this fascinating system.

## AUTHOR INFORMATION

### Corresponding Author

\*E-mail: ishi@tx.technion.ac.il.

### Author Contributions

The manuscript is based on the contributions of all authors. All authors have given approval to the final version of the manuscript.

### Notes

The authors declare no competing financial interest.

## ACKNOWLEDGMENTS

We thank Mrs. Berta Shdemati for her assistance in solution preparation and SAXS specimen preparation. We thank Mrs. Judith Schmidt for her help with cryo-TEM imaging, and Mr. Liron Issman for his assistance with cryo-SEM imaging and calculations of isooctane vapor pressure. We thank Mrs. Elinor Josef and Prof. Yachin Cohen for their superb assistance with the analysis and interpretation of SAXS results. This research was supported by The Israel Science Foundation (grant No. 659/11) and by the Technion Russell Berrie Nanotechnology Institute (RBNI).

## ABBREVIATIONS

PC, phosphatidylcholine  
PE, phosphatidylethanolamine  
PI, phosphatidylinositol



TEM, transmission electron microscope  
SEM, scanning electron microscope  
CEVS, controlled environment vitrification system  
cryo-, cryogenic  
rTLM, reverse threadlike micelle  
SAXS, small-angle X-ray scattering  
W/O, water in oil  
HR, high resolution

## REFERENCES

- (1) Evans, D. F.; Wennerstrom, H. In *The Colloidal Domain*; Wiley-VCH: New York, 1999.
- (2) Szuhaj, B. F., Ed. In *Lecithins: sources, manufacture & uses*; The American Oil Chemists Society: Champaign, IL, 1989.
- (3) Scartazzini, R.; Luisi, P. L. Organogels from Lecithins. *J. Phys. Chem.* **1988**, *92*, 829–833.
- (4) Schurtenberger, P.; Cavaco, C. Polymer-Like Lecithin Reverse Micelles. I. A Light Scattering Study. *Langmuir* **1994**, *10*, 100–108.
- (5) Schurtenberger, P.; Magid, L.; Lindner, P.; Luisi, P. In *A sphere to flexible coil transition in lecithin reverse micellar solutions*; Helm, C., Lösche, M., Möhwald, H., Eds.; Trends in Colloid and Interface Science VI; Springer: Berlin/Heidelberg, 1992; Vol. 89, pp 274–277.
- (6) Schurtenberger, P.; Scartazzini, R.; Luisi, P. L. Viscoelastic Properties of Polymerlike Reverse Micelles. *Rheol. Acta* **1989**, *28*, 372–381.
- (7) Schurtenberger, P.; Scartazzini, R.; Magid, L. J.; Leser, M. E.; Luisi, P. L. Structural and Dynamic Properties of Polymer-Like Reverse Micelles. *J. Phys. Chem.* **1990**, *94*, 3695–3701.
- (8) Shchipunov, Y. A.; Hoffmann, H. Thinning and Thickening Effects Induced by Shearing in Lecithin Solutions of Polymer-Like Micelles. *Rheol. Acta* **2000**, *39*, 542–553.
- (9) Angelico, R.; Ceglie, A.; Olsson, U.; Palazzo, G. Phase Diagram and Phase Properties of the System Lecithin-Water-Cyclohexane. *Langmuir* **2000**, *16*, 2124–2132.
- (10) Cavaco, C.; Schurtenberger, P. In *Viscoelastic lecithin reverse micelles: A simple model system for equilibrium polymers?*; Lagner, P., Glatter, O., Eds.; Trends in Colloid and Interface Science VII; Springer: Berlin/Heidelberg, 1993; Vol. 93, pp 202–203.
- (11) Peng, Q.; Luisi, P. L. The Behavior of Proteases in Lecithin Reverse Micelles. *Eur. J. Biochem.* **1990**, *188*, 471–480.
- (12) Avramiotis, S.; Papadimitriou, V.; Hatzara, E.; Bekiari, V.; Lianos, P.; Xenakis, A. Lecithin Organogels used as Bioactive Compounds Carriers. A Microdomain Properties Investigation. *Langmuir* **2007**, *23*, 4438–4447.
- (13) Angelico, R.; Ceglie, A.; Colafemmina, G.; Delfino, F.; Olsson, U.; Palazzo, G. Phase Behavior of the Lecithin/Water/Isooctane and Lecithin/Water/Decane Systems. *Langmuir* **2004**, *20*, 619–631.
- (14) Shchipunov, Y. A.; Hoffmann, H. Growth, Branching, and Local Ordering of Lecithin Polymer-Like Micelles. *Langmuir* **1998**, *14*, 6350–6360.
- (15) Cates, M. E. Reptation of Living Polymers: Dynamics of Entangled Polymers in the Presence of Reversible Chain-Scission Reactions. *Macromolecules* **1987**, *20*, 2289–2296.
- (16) Cates, M. E. Nonlinear Viscoelasticity of Wormlike Micelles (and Other Reversibly Breakable Polymers). *J. Phys. Chem.* **1990**, *94*, 371–375.
- (17) Wolf, G.; Kleinpeter, E. Pulsed Field Gradient NMR Study of Anomalous Diffusion in a Lecithin-Based Microemulsion. *Langmuir* **2005**, *21*, 6742–6752.
- (18) Avramiotis, S.; Cazianis, C. T.; Xenakis, A. Interfacial Properties of Lecithin Microemulsions in the Presence of Lipase. A Membrane Spin-Probe Study. *Langmuir* **1999**, *15*, 2375–2379.
- (19) Shchipunov, Y. A.; Hoffmann, H. Indicative Evidence for Coexistence of Long and Short Polymer-Like Micelles in Lecithin Organogel from Rheological Studies. *Langmuir* **1999**, *15*, 7108–7110.
- (20) Kumar, V. V.; Kumar, C.; Raghunathan, P. Studies on Lecithin Reverse Micelles: Optical Birefringence, Viscosity, Light Scattering, Electrical Conductivity, and Electron Microscopy. *J. Colloid Interface Sci.* **1984**, *99*, 315–323.
- (21) Talmon, Y. Staining and Drying-Induced Artifacts in Electron Microscopy of Surfactant Dispersions. *J. Colloid Interface Sci.* **1983**, *93*, 366–382.
- (22) Talmon, Y. In *Cryogenic Temperature Transmission Electron Microscopy in the Study of Surfactant Systems*; Binks, B. P., Ed.; Modern characterization methods of surfactant systems; Marcel Dekker: New York, 1999; pp 147–177.
- (23) Issman, L.; Talmon, Y. Cryo-SEM Specimen Preparation Under Controlled Temperature and Concentration Conditions. *Journal of microscopy* **2012**, *246*, 60–69.
- (24) Oostergetel, G. T.; Esselink, F. J.; Hadziioannou, G. Cryo-Electron Microscopy of Block Copolymers in an Organic Solvent. *Langmuir* **1995**, *11*, 3721–3724.
- (25) Danino, D.; Gupta, R.; Satyavolu, J.; Talmon, Y. Direct Cryogenic-Temperature Transmission Electron Microscopy Imaging of Phospholipid Aggregates in Soybean Oil. *J. Colloid Interface Sci.* **2002**, *249*, 180–186.
- (26) Behabtu, N.; Lomeda, J. R.; Green, M. J.; Higginbotham, A. L.; Sinitiskii, A.; Kosynkin, D. V.; Tsentlovich, D.; Parra-Vasquez, A. N. G.; Schmidt, J.; Kesselman, E.; Cohen, Y.; Talmon, Y.; Tour, J. M.; Pasquali, M. Spontaneous High-Concentration Dispersions and Liquid Crystals of Graphene. *Nat. Nanotechnol.* **2010**, *5*, 406–411.
- (27) Davis, V. A.; Parra-Vasquez, A. N. G.; Green, M. J.; Rai, P. K.; Behabtu, N.; Prieto, V.; Booker, R. D.; Schmidt, J.; Kesselman, E.; Zhou, W.; Fan, H.; Adams, W. W.; Hauge, R. H.; Fischer, J. E.; Cohen, Y.; Talmon, Y.; Smalley, R. E.; Pasquali, M. True Solutions of Single-Walled Carbon Nanotubes for Assembly into Macroscopic Materials. *Nat. Nano* **2009**, *4*, 830–834.
- (28) Bellare, J. R.; Davis, H. T.; Scriven, L. E.; Talmon, Y. Controlled Environment Vitrification System: An Improved Sample Preparation Technique. *J. Electron Microsc. Tech.* **1988**, *10*, 87–111.
- (29) Talmon, Y. In *Seeing giant micelles by cryogenic-temperature transmission electron microscopy (Cryo-TEM)*; Zana, R., Kaler, E. A., Eds.; Giant Micelles; CRC Press: New York, 2007; pp 163–178.
- (30) Lubovsky, M. Direct Imaging of Reverse Threadlike Micelles in Non-Aqueous Systems, M.Sc. thesis, 2008.
- (31) Koifman, N. Nanostructure in Non-Aqueous Solutions, M.Sc. thesis, Technion, Haifa, 2012.
- (32) Percus, J. K.; Yevick, G. J. Analysis of Classical Statistical Mechanics by Means of Collective Coordinates. *Phys. Rev.* **1958**, *110*, 1–13.
- (33) Vrij, A. Mixtures of Hard Spheres in the Percus–Yevick Approximation. Light Scattering at Finite Angles. *J. Chem. Phys.* **1979**, *71*, 3267–3270.
- (34) Alexandridis, P.; Olsson, U.; Lindman, B. A Record Nine Different Phases (Four Cubic, Two Hexagonal, and One Lamellar Lyotropic Liquid Crystalline and Two Micellar Solutions) in a Ternary Isothermal System of an Amphiphilic Block Copolymer and Selective Solvents (Water and Oil). *Langmuir* **1998**, *14*, 2627–2638.
- (35) Alexandridis, P.; Olsson, U.; Lindman, B. A Reverse Micellar Cubic Phase. *Langmuir* **1996**, *12*, 1419–1422.
- (36) Seddon, J. M.; Bartle, E. A.; Mingins, J. Inverse Cubic Liquid-Crystalline Phases of Phospholipids and Related Lyotropic Systems. *J. Phys.: Condens. Matter* **1990**, *2*, SA285–SA290.
- (37) Seddon, J. M.; Templer, R. H. Cubic Phases of Self-Assembled Amphiphilic Aggregates. *Philos. Trans.: Phys. Sci. Eng.* **1993**, *344*, 377–401.
- (38) Luzzati, V.; Vargas, R.; Gulik, A.; Mariani, P.; Seddon, J. M.; Rivas, E. Lipid Polymorphism: A Correction. the Structure of the Cubic Phase of Extinction Symbol Fd- Consists of Two Types of Disjointed Reverse Micelles Embedded in a Three-Dimensional Hydrocarbon Matrix. *Biochemistry (N. Y.)* **1992**, *31*, 279–285.
- (39) Ben-Barak, I.; Talmon, Y. Direct-Imaging Cryo-SEM of Nanostructure Evolution in Didodecyltrimethylammonium Bromide-Based Microemulsions. *Z. Phys. Chem.* **2012**, *226*, 665–674.
- (40) Hoeller, S.; Klang, V.; Valenta, C. Skin-Compatible Lecithin Drug Delivery Systems for Fluconazole: Effect of Phosphatidylethanol-

amine and Oleic Acid on Skin Permeation. *J. Pharm. Pharmacol.* **2008**, *60*, 587–591.

(41) Koetz, J.; Saric, M.; Kosmella, S.; Tiersch, B. Influence of Polyelectrolytes on Lecithin-Based W/O Microemulsions and BaSO<sub>4</sub>-Nano Particle Formation. *Prog. Colloid Polym. Sci.* **2004**, *129*, 95–104.

(42) Zheng, Y.; Lin, Z.; Zakin, J. L.; Talmon, Y.; Davis, H. T.; Scriven, L. E. Cryo-TEM Imaging the Flow-Induced Transition from Vesicles to Threadlike Micelles. *J. Phys. Chem. B* **2000**, *104*, 5263–5271.